



## Stability and Thermodynamic Consistency in the Coexistence Curve Of Liquid-Vapor in A Modified Pseudo-Potential Model

M. Taghilou\*, S. Zarei

Department of Mechanical Engineering, University of Zanjan, Zanjan, Iran

**ABSTRACT:** In this paper, the conditions of convergence and thermodynamic consistency of the Kupershtokh model for simulating a 2D droplet are investigated. Hence, the coexistence curve of liquid and vapor phases is divided into four levels according to the constant of the potential function,  $k$  and the weight coefficient of the intermolecular forces,  $A$ . Accordingly, a range is reported for  $k$  at each level. This range for level 1 with the lowest density ratio is  $k_{\min} = 0.05$  to  $k_{\max} = 0.22$  and for the fourth level with the highest density ratio is  $k_{\min} = 0.002$  to  $k_{\max} = 0.01$ . Also, the appropriate weight coefficient for intermolecular forces,  $A_{fit}$  is obtained for yielding the thermodynamic consistency at levels 1 to 4 equal with 0.25, 0.025, -0.082 and -0.125, respectively. Results show that the choice of  $A=0.5$  produces symmetric and  $A=0$  causes asymmetric forces in the interface. Finally, the problem of mass conservation in four levels is investigated. Results show that Kupeshtokh model has a better behavior in controlling the mass of the droplet in the high density ratios. So, the change in the mass of the droplet at level 1 is more than 20% and at the level of 4 is less than 1%.

### Review History:

Received:

Revised:

Accepted:

Available Online:

### Keywords:

Lattice Boltzmann method

Pseudo-potential model

Coexistence curve

Intermolecular forces

### 1- Introduction

The most common model for simulating two-phase flows in the lattice Boltzmann framework is the pseudopotential model [1]. The emergence of spurious velocities, thermodynamic inconsistency, the low viscosity, and density ratios and the relation between the equation of state and surface tension are among the limitations of this model [2].

Kupershtokh model [3] succeeds to reduce spurious velocities and achieve a high-density ratio by first, using the Exact Difference Method (EDM) in force insertion and second, the combination of symmetric and non-symmetric methods in the calculation of the potential function at the interface of the two phases. However, the results of this model are highly dependent on the behavior of the potential function, which is controlled by the constant of potential function,  $k$ , and the weighting factor of the force equation,  $A$ . In this paper, in addition to providing a pattern for selecting the constant of the potential function and the weight factor of the force, the force distribution conditions at the interface of the two phases are studied.

### 2- Methodology

#### 2- 1- Lattice Boltzmann method

In order to apply the external forces to the Boltzmann equation, one can write [4]:

$$f_i(\mathbf{x} + \mathbf{c}_i \Delta t, t + \Delta t) = f_i(\mathbf{x} + \mathbf{c}_i \Delta t, t) - \frac{\Delta t}{\tau} [f_i(\mathbf{x} + \mathbf{c}_i \Delta t, t) - f_i^{eq}(\mathbf{x} + \mathbf{c}_i \Delta t, t)] + \Delta f_i \quad (1)$$

In Eq. (1),  $\Delta f_i$  is due to the external forces. In this paper, the exact difference method for the application of external forces is used. In this method, the difference in the equilibrium distribution function before and after force application in a time step is defined as follows [3]:

$$\Delta f_i(\mathbf{x}, t) = f_i^{eq}(\rho(\mathbf{x}, t), \mathbf{u} + \Delta \mathbf{u}) - f_i^{eq}(\rho(\mathbf{x}, t), \mathbf{u}) \quad (2)$$

where,  $\Delta \mathbf{u} = \mathbf{F} \Delta t / \rho$ .

#### 2- 2- Pseudopotential model

In order to calculate the intermolecular forces, the gradient of the potential function  $\tilde{U}$  must be taken according to  $\mathbf{F} = -\nabla \tilde{U}$ . For this purpose, two solutions are proposed. In the first solution, the gradient is computed proportional to the directions of the D2Q9.

$$\mathbf{F} = \frac{1}{2\alpha \Delta x} \sum_{k=1}^N \frac{G_k}{G_1} \tilde{U}(\mathbf{x} + \mathbf{c}_k) \mathbf{c}_k \quad (3)$$

In Eq. (3),  $G_k / G_1$  is a coefficient that shows the contribution of adjacent points in the calculation of  $\nabla \tilde{U}$ . The  $G_k$

\*Corresponding author's email: taghilou@znu.ac.ir



coefficient for the main directions is equal to G1 and in the minor directions is 0.25 G1. In the second solution, with the definition of the special function, one can consider the potential function as follows [5-7]:

$$\phi(\rho_r, T_r) = \sqrt{-\tilde{U}(\rho_r, T_r)} \quad (4)$$

Substituting Eq. (4) in  $\mathbf{F} = -\nabla\tilde{U}$  the following equation is obtained [3]:

$$\mathbf{F} = 2\phi\nabla\phi \quad (5)$$

Using numerical approximation, Eq. (5) can be written as [5, 7]:

$$\mathbf{F} = \frac{1}{\alpha\Delta x} \phi(\mathbf{x}) \sum_{k=1}^N \frac{G_k}{G_1} \phi(\mathbf{x} + \mathbf{c}_k) \mathbf{c}_k \quad (6)$$

The following equation can be obtained by combining Eqs. (3) and (6) with different weights [3]:

$$\mathbf{F} = \frac{1}{\alpha\Delta x} \left[ \begin{array}{l} A \sum_{k=1}^N \frac{G_k}{G_1} \phi^2(\mathbf{x} + \mathbf{c}_k) \mathbf{c}_k + \\ (1-2A)\phi(\mathbf{x}) \sum_{k=1}^N \frac{G_k}{G_1} \phi(\mathbf{x} + \mathbf{c}_k) \mathbf{c}_k \end{array} \right] \quad (7)$$

In Eq. (7), parameter A acts as a weighting factor. Eq. (7) for the value of A=0 leads to Eq. (6), and for A=0.5 leads to Eq. (3).

### 3- Results and Discussion

To check the accuracy and obtain the surface tension the Laplace test is carried out. According to Laplace's law, the difference in pressure inside and outside of a two-dimensional droplet is obtained by [8]:

$$\Delta p = p_{in} - p_{out} = \frac{\sigma}{R} \quad (8)$$

The results of Eq. (8) in a 200x200 computational domain are obtained from two equations of states of van der Waals and modified Kaplun-Meshalkin and are shown in Figs. 1 and 2..., show the coexistence curve which is obtained by Maxwell equal area using van der Waals equation of state. According to this figure, it is seen that by increasing the density ratio access to a pattern will be necessary to select the simulation parameters of the flow. Accordingly, the temperature range of 0.92-0.99 is named as level 1, the range of 0.7-0.9 named as level 2, the range of 0.5-0.65 refers to level 3 and a temperature range of 0.3-0.45 is known as level 4.

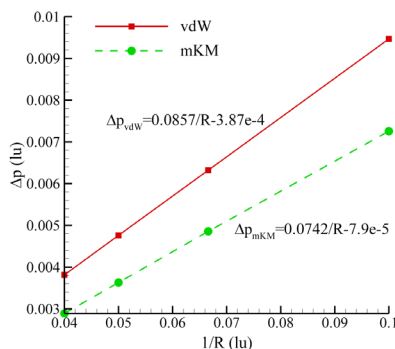


Fig. 1. Laplace test to calculate the surface tension of the droplet.

### 3- 1- Effect of k on the coexistence curve

Changing the parameter k shows that for each  $T_r$ , there is a range of k, that the convergence of the solution cannot be reached outside it. The lower limit of this domain is  $k_{min}$  and its upper limit is  $k_{max}$ . As shown in Fig. 2, the  $k_{min}$  and  $k_{max}$  values are different for each level. By increasing the density ratio these values decreased from 0.05 to 0.002 for  $k_{min}$  and from 0.22 to 0.01 for  $k_{max}$ , respectively.

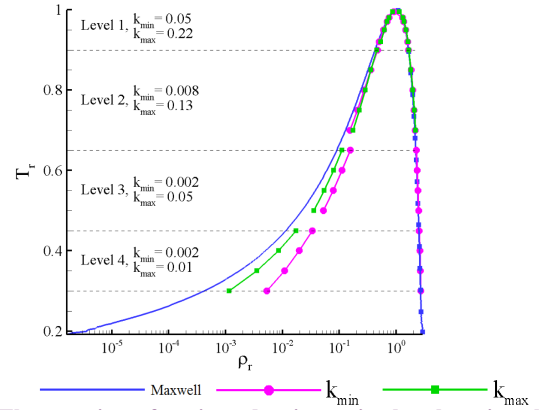


Fig. 2. The creation of various density ratios by changing the parameter of k.

### 4- 4.2. Effect of A on the coexistence curve

In this section, the value of k is equal to  $k_{max}$  at each level. Fig. 3 shows the variations in the density of the liquid and vapor phases in terms of the  $T_r$  at four levels of 1 to 4. On this basis, it is seen that by changing the value of A, the conditions for convergence of simulations are provided in  $A_{min} < A < A_{max}$ . In this range,  $A_{min}$  represents the lower limit of A for the lowest density ratio, and  $A_{max}$  represents the upper limit of A for the highest density ratio. The important point in this section is the introduction of conditions in which the numerical density ratio is equal to the theory of Maxwell's equal area. In other words, by choosing the proper amount of  $A_{fit}$ , one can achieve the thermodynamic consistency in simulating a two-dimensional droplet.

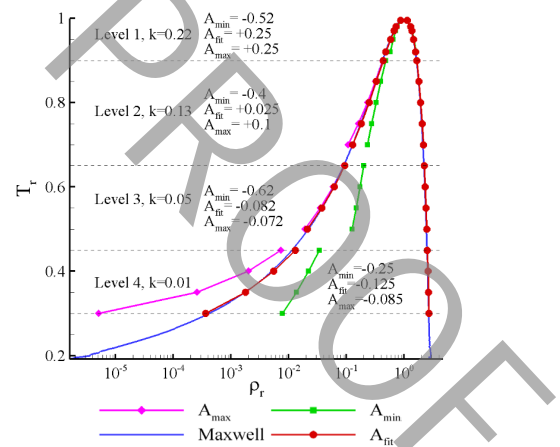


Fig. 3. Matching the numerical density ratio with the Maxwell theory by changing the weighting factor of A.

### 5- Conclusion

• By increasing the density ratio, the stability domain of the solution is transmitted to smaller values of k. So that, the

$k_{\min}=0.05$  at level 1 is reduced to 0.002 in the fourth level and the value of  $k_{\max}$  reduces from 0.22 in level 1 to 0.01 in level 4.

• Changing the weight factor of  $A$  causes a change in the density ratio of the two phases. These changes are such that by choosing the appropriate value for  $A_{\text{fit}}$ , one can obtain the density ratio corresponding to the base of the Maxwell equal area.

## 6- References

- [1] X. Shan, H. Chen, Lattice Boltzmann model for simulating flows with multiple phases and components, *Physical Review E*, 47(3) (1993) 1815.
- [2] L. Chen, Q. Kang, Y. Mu, Y.-L. He, W.-Q. Tao, A critical review of the pseudopotential multiphase lattice Boltzmann model: Methods and applications, *International journal of heat and mass transfer*, 76 (2014) 210-236.
- [3] A. Kupershtokh, D. Medvedev, D. Karpov, On equations of state in a lattice Boltzmann method, *Computers & Mathematics with Applications*, 58(5) (2009) 965-974.
- [4] K. Timm, H. Kusumaatmaja, A. Kuzmin, *The lattice Boltzmann method: principles and practice*, in, Springer: Berlin, Germany, 2016.
- [5] A. Kupershtokh, C. Stamatelatos, D. Agoris, Stochastic model of partial discharge activity in liquid and solid dielectrics, in: *IEEE International Conference on Dielectric Liquids, 2005. ICDL 2005.*, IEEE, 2005, pp. 135-138.
- [6] A.L. Kupershtokh, Simulation of flows with vapor-liquid interfaces using lattice Boltzmann equation method, *Siberian Journal of Pure and Applied Mathematics*, 5(3) (2005) 29-42.
- [7] A. Kupershtokh, D. Karpov, D. Medvedev, C. Stamatelatos, V. Charalambakos, E. Pyrgioti, D. Agoris, Stochastic models of partial discharge activity in solid and liquid dielectrics, *IET Science, Measurement & Technology*, 1(6) (2007) 303-311.
- [8] H. Deng, K. Jiao, Y. Hou, J.W. Park, Q. Du, A lattice Boltzmann model for multi-component two-phase gas-liquid flow with realistic fluid properties, *International Journal of Heat and Mass Transfer*, 128 (2019) 536-549.